

### Chapter 3: In situ crystallization of fluoride-mediated, pure-silica zeolite thin films

#### Abstract

Two methods for the synthesis of fluoride-mediated, zeolite thin films were examined to determine if they could overcome the common limitations of fluoride-mediated zeolite syntheses, which are frequently incompatible with standard film synthesis techniques.

The first method utilised a seeding and dilution modification to typical *in situ* film syntheses. The second method applied the vapor phase transport method to the zeolite mineralizing agent, fluoride, to crystallize a precursor film deposited by dip-coating techniques. With this method, we obtained thin films of silicate and germanosilicate zeolites with the LTA topology on a variety of substrates. The films were characterized by a combination of X-ray diffraction, field emission scanning electron microscopy, X-ray energy dispersive analyses, and mechanical testing via nanoindentation. The films were polycrystalline, inter-grown, continuous, and well-adhered to their substrates. The vapor phase transport of fluoride is a facile and general method for the synthesis of fluoride-mediated, zeolite thin films, specifically those with the pure-silica composition, and could extend the current library of zeolite films available.

Reproduced in part with permission from H. K. Hunt, C. M. Lew, M. Sun, Y. Yan and M. E. Davis, Pure-Silica Zeolite Thin Films by Vapor Phase Transport of Fluoride for Low-k Applications, *Microporous Mesoporous Mat.* © 2009 Elsevier.

## 1. Introduction

There is growing enthusiasm for the use of pure-silica zeolite (PSZ) films in applications such as chemical sensors, membrane reactors, and microelectronic devices.<sup>1,2,3,4,5,6,7,8,9</sup>

For instance, the development of pure-silica zeolite thin films as low dielectric constant (low- $k$ ) materials is of particular interest to the semiconductor industry. Attempts to decrease feature size in microprocessors have been met with potential increases of cross-talk noise and energy dissipation. In order to overcome such limitations in an integrated circuit with feature sizes of 14 nm or smaller, an ultra-low- $k$  material (between 2.3 – 2.6) must be developed to replace nonporous silica ( $k = 4.0$ ) as the dielectric film insulating the wiring between transistors.<sup>10</sup> Typical approaches to the creation of low- $k$  materials involve the introduction of porosity via methods such as sol-gel processing, surfactant-templating, and zeolite crystallization. Sol-gel-derived and surfactant-templated mesoporous silicas, however, tend to have low mechanical stiffness and high hydrophilicity.<sup>11,12,13</sup> In contrast, pure-silica zeolites are crystalline, porous structures with high mechanical strength, and high heat conductivity, as well as high thermal and chemical stability.<sup>14,15</sup> Additionally, the variety of zeolite topologies enables production of a tunable  $k$ -value by selecting topologies with different porosities. The porosity of a given zeolite is a function of its framework density (FD, the number of tetrahedrally-coordinated atoms per 1000 Å<sup>3</sup>); for instance, the LTA topology first produced in pure-silica form by Corma et al. in 2004 has the lowest framework density (FD = 14.2) among all available pure-silica zeolites, and therefore could have the lowest dielectric constant.<sup>16,17</sup> For the reasons mentioned, the exploration of low-framework density pure-silica zeolites as low- $k$  dielectric materials has generated great interest. However, these

efforts have been limited by the number of pure-silica zeolite materials that can be accessed via current zeolite thin film synthetic approaches, such as *in situ* crystallization, and the spin-on of zeolite nanoparticle suspensions. (*In situ* crystallization refers to a process where the zeolite film is grown *in situ* onto a bare substrate from a dilute precursor solution that is free from preformed crystals.) Indeed, of the 19 zeolite topologies with pure-silica compositions, only 4 (structure codes MFI (FD = 18.4,  $k = 2.7$  via *in situ* crystallization and spin-coating), MEL (FD = 17.4,  $k = 1.9$  via spin-coating, 1.51 via spin-coating followed by hydrofluoric acid-resistant modifications), \*MRE (FD = 19.8,  $k = 2.7$  via vapor phase transport), and BEA\* (FD = 15.3,  $k = 2.3$  via *in situ* crystallization, 2.07 via secondary growth)) have been prepared into films for zeolite low- $k$  applications.<sup>15,18,19,20,21,22</sup>

Pure-silica zeolites can be synthesized from compositions that contain fluoride ions.<sup>23,24</sup> These fluoride-mediated syntheses produce the most promising candidates for low- $k$  pure-silica zeolites materials, because they generally have low framework density and low silanol defect density when compared to pure-silica zeolites made using hydroxide as the mineralizing agent (such as the aforementioned films of MFI and MEL). However, the syntheses of fluoride-mediated zeolites have several features that are incompatible with current film *in situ* and spin-on deposition approaches. First, the extremely low  $\text{H}_2\text{O} / \text{SiO}_2$  ratios ( $\sim 2 - 7$ ) required for crystallization prevents transport of reactants, such as the organic structure-directing agent (SDA) and mineralizing agent ( $\text{F}^-$ ), from the bulk gel to the substrate through solvent mediation, and prevents good adhesion of material to the substrate. Second, the presence of the fluoride ion in the gel tends to cause severe

corrosion on direct contact with the substrate. Third, the synthesis conditions are not conducive to producing nanocrystals suitable for spin-on processes. When attempts are made to use *in situ* crystallization procedures to make films of fluoride-mediated zeolites, such as the pure-silica BEA\*-type solids mentioned previously and aluminum-free LTA (the germanosilicate composition of LTA), the resulting films can suffer from poor adhesion to the substrate and are difficult to reproduce reliably. Similarly, seeded synthetic methods like secondary growth, such as the production of thin films of pure-silica BEA\* may be limited by the production of zeolite nanocrystals. The combination of these factors has made producing thin films of fluoride-mediated, pure-silica zeolites very difficult.

Resolving the aforementioned issues requires modification of current film synthesis techniques. To this end, we investigate two types of modifications to typical *in situ* crystallization routes that may overcome the limitations of fluoride-mediated syntheses: (1) the seeding and diluting of the zeolite precursor gel (Figure 3.1), and (2) the vapor phase transport of fluoride (Figure 3.2). Our interest is primarily in *in situ* techniques because these methods yield films of fully-intergrown crystals, which allows us to measure the intrinsic properties of the material, rather than the those of a composite material. To determine the viability of these two modifications, we applied them separately to the fluoride-mediated syntheses of zeolite LTA. Fluoride-mediated LTA was chosen as the test subject for this demonstration for the following reasons: (1) when made with fluoride, it can be made in both the pure-silica and the aluminum-free (germanosilicate) composition, which demonstrates whether the modifications are

applicable to a range of chemical compositions, (2) the synthesis of the pure-silica form requires the use of two structure-directing agents, making it one of the more difficult syntheses to reproduce, (3) the use of the LTA topology in its aluminosilicate form for its ion-exchange and water-softening properties represents the largest world-wide use of any zeolite, and (4) the pure-silica LTA structure has the lowest framework density of the known pure-silica zeolites and therefore, a film of this material could prove extremely useful for low- $k$  applications. Additionally, a variety of *in situ* films techniques have been studied previously for the hydroxide-mediated, aluminosilicate LTA material, which provides insight into problems that might arise during film synthesis with the LTA structure. Therefore, the fluoride-mediated LTA materials are of great interest both in terms of end use and the difficulty of the synthesis. In this chapter, we discuss the results and effectiveness of these two modifications to the *in situ* film crystallization procedures.

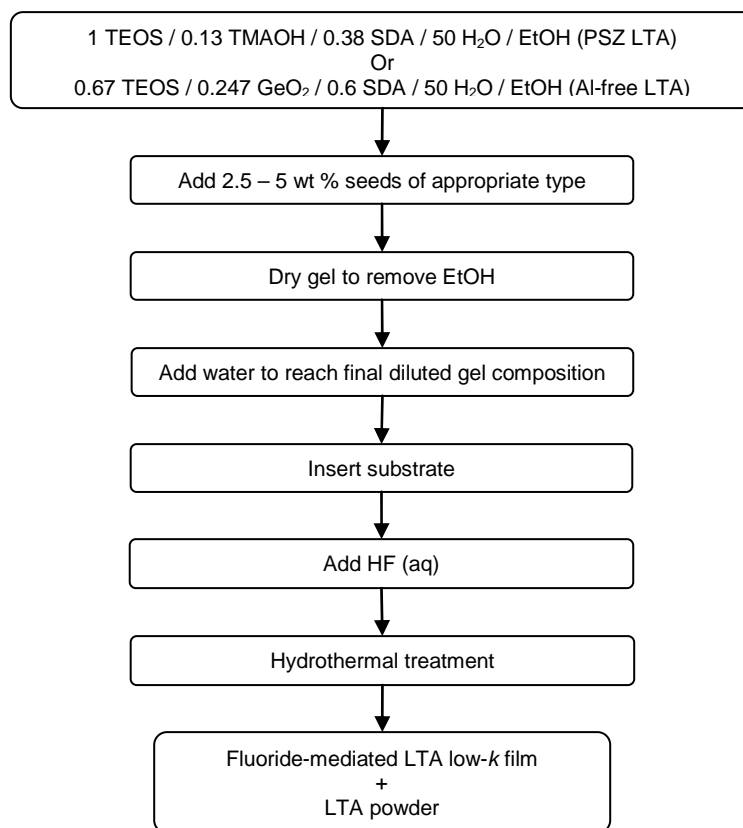


**Figure 3.1** Schematic of the synthesis process of fluoride-mediated zeolite films by the seeding / diluting modification to in situ crystallization

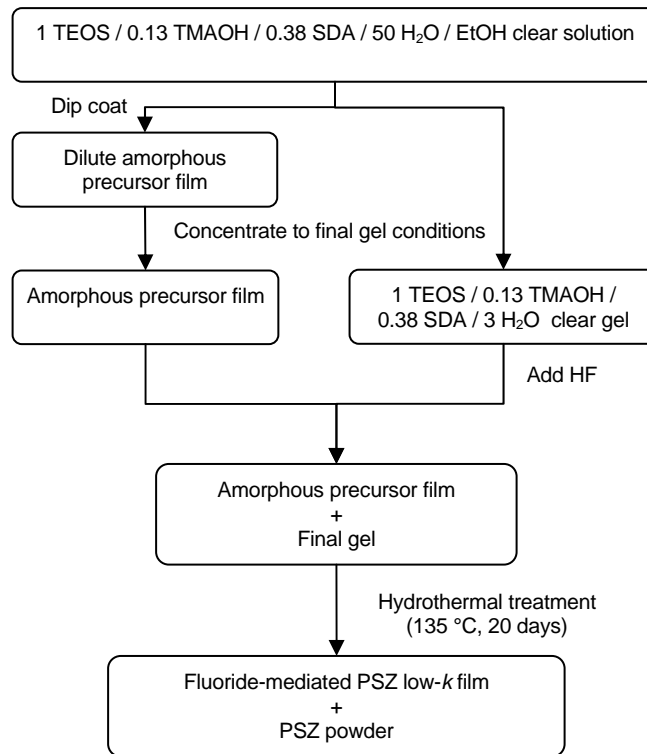


**Figure 3.2** Schematic of the synthesis process of fluoride-mediated, pure-silica zeolite LTA films by the vapor phase transport of fluoride

## 2. Results and Discussion

The key to a film deposition method applicable to fluoride-mediated zeolites is to accommodate the common aspects of their powder syntheses: (1) tetraethylorthosilicate (TEOS) is the liquid silica source that is hydrolyzed for several hours to produce the source of silica, (2) the hydrolysis of TEOS requires excess water that must be removed from the gel prior to crystallization, (3) the final gel is usually very concentrated and extremely dry, and (4) hydrofluoric acid is used as the mineralizing agent, and is added to the gel just prior to crystallization. Additionally, many zeolite gels may be seeded to encourage growth of zeolite crystals of a specific phase, a step that detaches the nucleation and crystal growth mechanisms of zeolite formation, as discussed in Chapter 1. To overcome the limitations of a lack of bulk transport of the zeolite precursor gel to the substrate surface, we must take advantage of either the ability to seed the precursor gel, which promotes growth of a pure phase of LTA, or of the time when the zeolite gel is dilute. The seeding / diluting modification takes advantage of the first, while the vapor phase transport of fluoride modification takes advantage of the second.

### 2.2 Seeding and Diluting the Zeolite Precursor Gel

Shortly after the introduction by Corma et al. of the pure-silica ITQ-29 (LTA topology) in 2004, Bouiza et al. demonstrated that, although the synthesis of pure-silica LTA is often difficult to repeat because of the difficulties of a fluoride-mediated synthesis that uses not one, but two structure-directing agents, the zeolite synthesis for high silicon-to-aluminum ratios could be greatly simplified by the addition of pre-formed LTA seeds.<sup>25</sup>



For instance, the LTA synthesis described by Corma et al. often resulted in a mixed LTA / AST zeolite phase if any of the conditions in the synthesis were even slightly off the described procedure. The addition of LTA seeds allowed the synthesis of the pure LTA phase to proceed repeatably, even when the synthesis conditions were slightly incorrect. This approach intrigued us, because seeding the zeolite precursor gel prior to hydrothermal treatment could allow us to also dilute the gel to conditions under which ITQ-29 does not typically form. Dilution of the gel would then solve the transport and adhesion limitation problems. Therefore, we modified the standard in situ crystallization protocols to include seeding the zeolite precursor gel with previously-made ITQ-29 seeds, diluting the zeolite gel by adding excess distilled, de-ionized water, and subjecting the gel to hydrothermal treatment in the presence of a substrate. The experimental ranges for the seed amount are 2.5 - 20 wt % of the amount of silica present in the zeolite gel, and for the water-to-silica ratio are 10 - 200 (germanosilicate phase) and 2 - 50 (pure-silica zeolite phase), as shown in Figures 3.3 and 3.4, below. Using this method over a wide range of synthesis conditions demonstrated that while the modifications to the in situ crystallization protocols did result in the formation and growth of the desired ITQ-29 composition in the bulk zeolite gel and powder, even at high dilutions (which was gratifying, as it increases the flexibility of the conditions under which ITQ-29 could form), it did not produce films of any quality on the substrate.

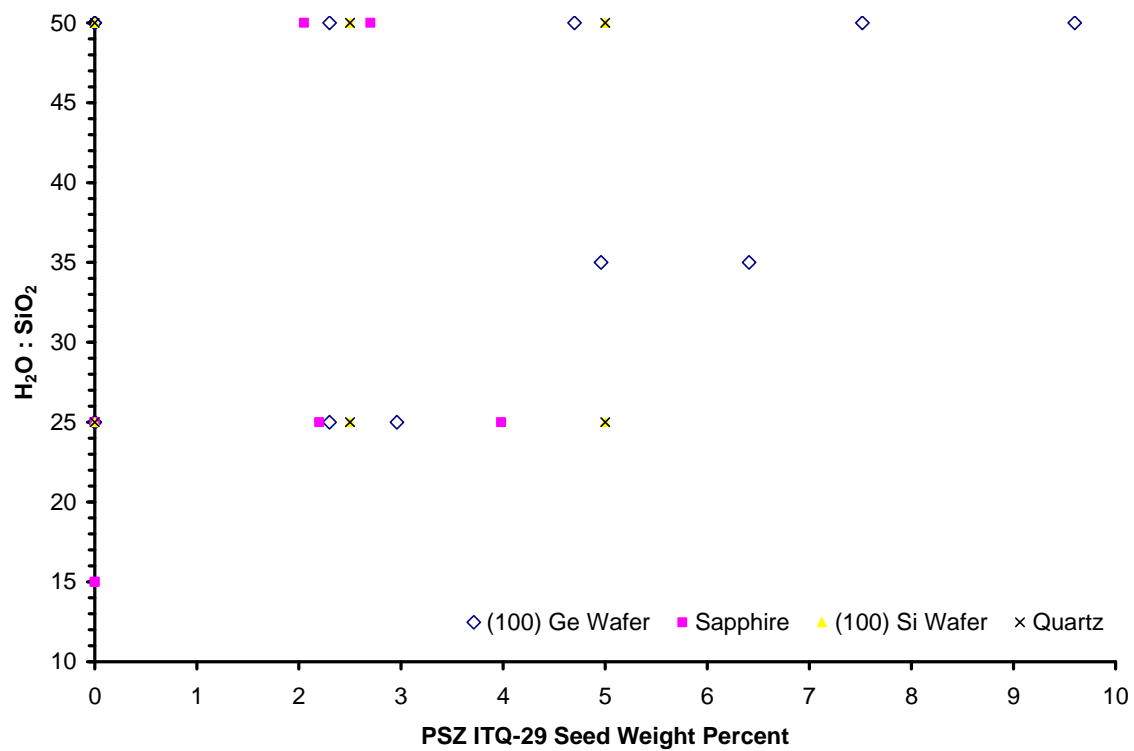


**Figure 3.3** PSZ ITQ-29 (LTA) film synthesis attempts using various substrates, seed amounts, and dilutions

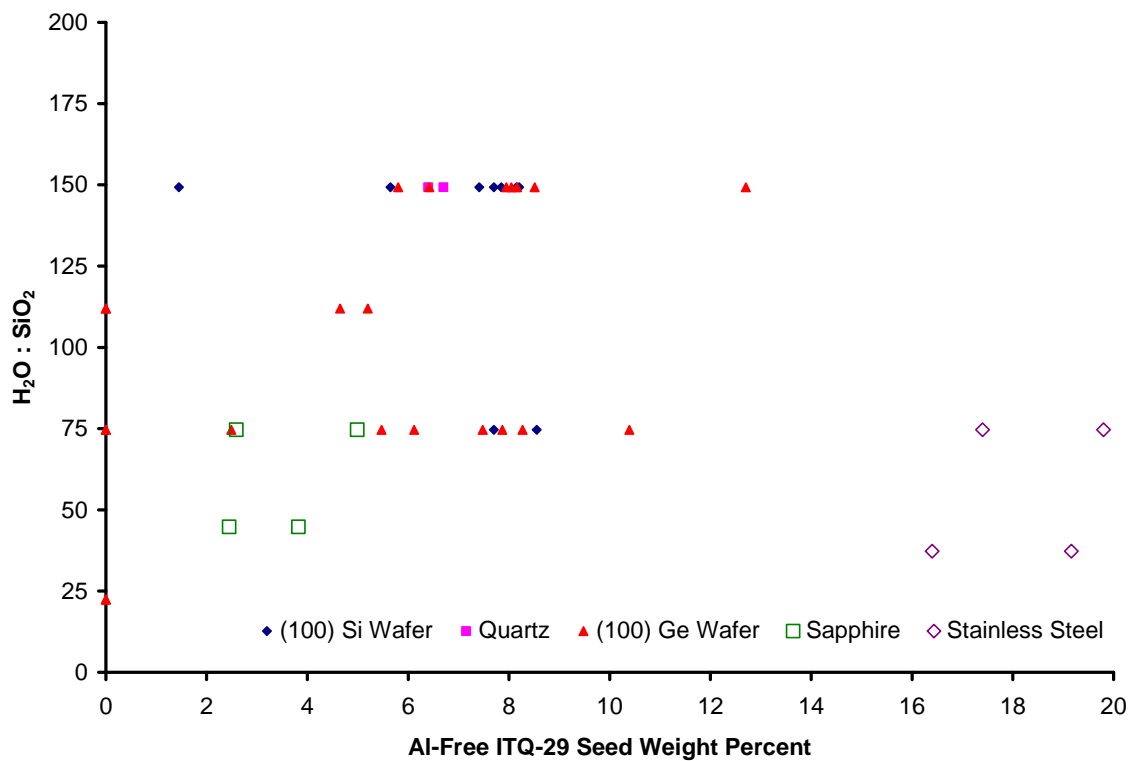


**Figure 3.4** Al-free ITQ-29 (LTA) film synthesis attempts using various substrates, seed amounts, and dilutions

Low dilution and high seed amounts generally resulted in more favorable conditions for the development of ITQ-29 crystals in the bulk zeolite gel, but did not promote transport of nucleated zeolite crystals from the bulk gel to the support, nor did they promote nucleation on the surface of the substrate. The supports inspected for their viability as substrates included (100) Si, (100) Ge, sapphire ( $\text{Al}_2\text{O}_3$  in a corundum topology, without impurities), stainless steel, and quartz. Additionally, the dilution of the zeolite precursor gel resulted in a slurry when the aqueous hydrofluoric acid was added, instead of the hoped-for clear solution. The presence of the hydrofluoric acid in the diluted bulk zeolite precursor gel also presented problems during crystallization, as the acid readily attacked the surface of the substrate, leading to leaching of the substrate into the bulk, and destroying the substrate itself. For instance, the (100) Si wafers, which had one polished side, frequently were blackened, pocked, and very brittle after hydrothermal treatment in the gel. The substrate itself also presented challenges to ITQ-29 formation, whether in the bulk or on the surface, because material from the substrate leaches very easily into the bulk gel, which adversely affected the gel composition, especially in the case of the stainless steel substrate. The presence of aluminum in the ITQ-29 syntheses, even in small amounts, and with seeds present, significantly reduced the ability of the ITQ-29 material to form. These results demonstrated that, although seeding and diluting the zeolite precursor gel increased the range of acceptable conditions for the synthesis ITQ-29 beyond what has been reported in literature, the modification did not fully address the problems associated with the fluoride-mediated, thin film syntheses.

### 2.3 Vapor Phase Transport of Fluoride

Traditionally, VPTM has been used to create membranes of aluminosilicate zeolites on porous alumina substrates by first covering the support by submersion in a parent gel containing alumina, silica, water, and the mineralizing agent, and then crystallizing the covered substrate hydrothermally in the presence of SDA and water in the vapor phase (the remaining parent gel not used for coating is not crystallized).<sup>26</sup> This process has been used to produce non-fluoride-mediated, pure-silica zeolite films of ZSM-48 (\*MRE), for example. More recently, Matsukata and co-workers have extended this approach by incorporating the silica source in the vapor phase, rather than the SDA and solvent.<sup>27</sup> The traditional VPTM is not directly suited to fluoride-mediated zeolite film formation for the reasons mentioned previously regarding the unsuitability of standard *in situ* and spin-on techniques, but it does have some aspects that may be modified to fluoride syntheses. Traditional VPTM syntheses require a clear solution *containing the mineralizing agent* into which the substrate may be submerged, resulting in a loosely adhered coating. The only time a clear solution is present during a fluoride-mediated zeolite synthesis is during the hydrolysis of TEOS – prior to the addition of the mineralizing agent. After hydrolyzing, the water is evaporated from the gel, thus beginning the concentration of the gel to the required water content. We, therefore, modified the VPTM to take advantage of the time the gel is actually dilute - *prior to evaporation and addition of the mineralizing agent*. We deposited the amorphous precursor film by dipcoating of the dilute solution right after hydrolysis, before the precursor concentration (Figure 3.5).

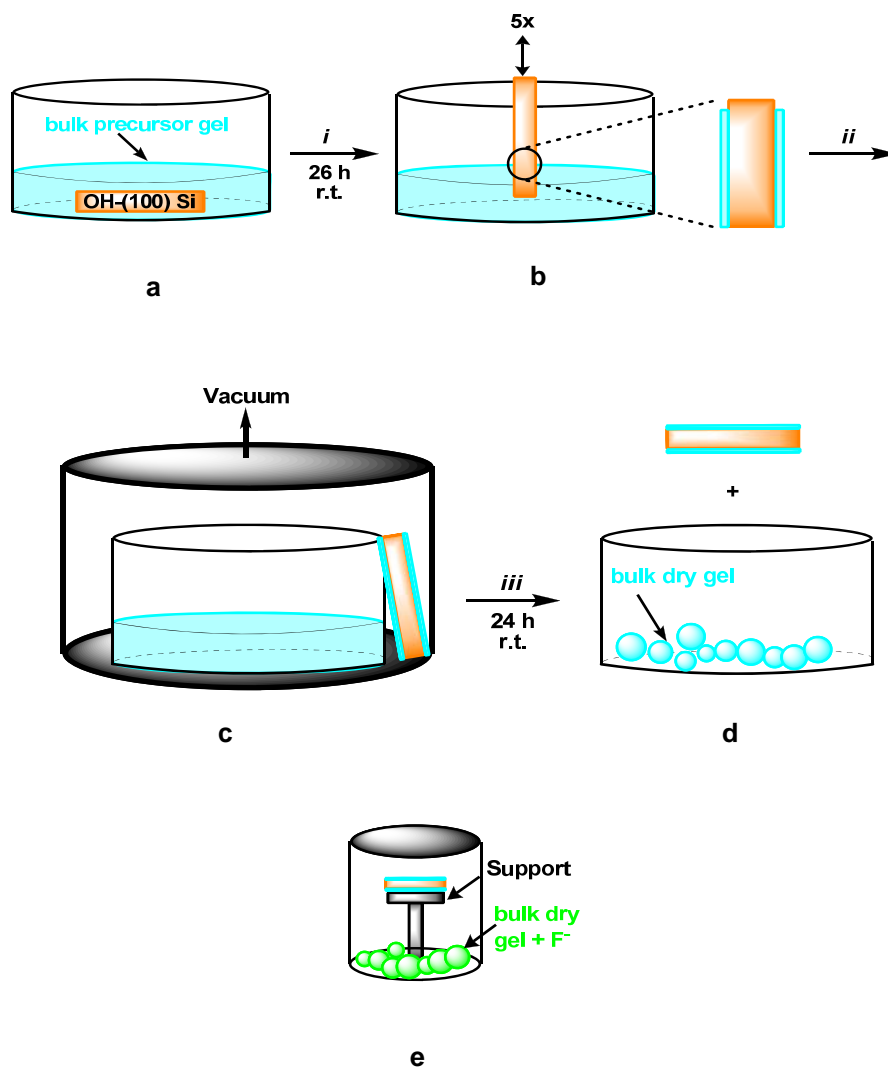


**Figure 3.5** (a) Substrate submerged in ITQ-29 precursor gel of appropriate molar composition, (i) Stir to hydrolyze the TEOS; (b) Substrate subjected to dip-coating, (ii) Dip-coat substrates, 5x, in the hydrolyzed gel to create amorphous precursor film; (c) Coated substrate and bulk precursor gel placed inside vacuum desiccator, (iii) Evaporate ethanol produced during hydrolysis and excess H<sub>2</sub>O; (d) Amorphous precursor film and solid (dry) gel; (e) Introduce dry gel into Teflon®-lined Parr Autoclave after addition of HF (aq) to dry gel, introduce coated substrate (no HF present in amorphous film) into autoclave on elevated Teflon® platform, and crystallize via VPTM

Our new methodology for the synthesis of pure-silica zeolite films involves the dip-coating of the prepared substrate in a hydrolized parent gel *prior to evaporation and addition of the mineralizing agent*, and an ethanol/water evaporation step that is conducted in a low-temperature oven or at room temperature to adhere an amorphous film of that gel to the substrate. This low-temperature process prevents crack formation during evaporation of the excess solvent, a common problem with the coating process in the VPTM.<sup>26</sup> To prevent the amorphous films from flaking off the substrate, the native oxide layer present on the substrate is replaced with silanols via successive HF / piranha dips prior to dip-coating the substrate. This increases the hydrophilicity of the substrate and improves adhesion between the substrate and the amorphous precursor film. Dip-coating at this point also allows the final film thickness to be modified based on the number of coats; similarly, spin-coating could also be used to ensure repeatable, tunable film thicknesses. Note that dip-coating results in a substrate coated on both sides, and a final film on both sides of the substrate. After dip-coating and evaporating excess solvent, a solution of HF (aq) is then added to the dry bulk gel (not the dip-coated precursor film), which is mixed, and then introduced into a Teflon®-lined, Parr Autoclave. The coated substrate is placed on an elevated, Teflon® platform inside the autoclave to prevent contact with the fluoride-containing bulk gel. Crystallization of the film and bulk gel proceeds using temperatures reported in the literature from synthesis of powdered samples.

It should be noted that crystallizing the bulk gel with the coated substrate leads to a low process economy; however, we found that we could crystallize up to five films at once

(limited by the space in the Teflon liner) using one synthesis gel. It should also be possible to crystallize the substrate coating using only the aqueous solution of hydrofluoric acid in the liner, if the appropriate ratio of acid to gel coating is used. However, we did not investigate this, and instead used the presence of the bulk gel as a mediation tool for obtaining the correct ration of reagents. Note that, unlike the traditional VPTM, neither the solvent or the SDA is introduced purposefully to the amorphous precursor film via the vapor phase. Instead, we take advantage of the volatile nature (in the form of HF gas) of the mineralizing agent ( $F^-$ ), and its transport via the vapor phase. It is possible that some amount of the other reagents in the bulk transfer via the vapor phase, but without the transport of the fluoride, the films would not crystallize. The vapor phase transport of the mineralizing agent prevents etching of substrate surfaces from direct contact with the aqueous hydrofluoric acid. Presumably, at long crystallization times, the  $F^-$  is present in three phases: the bulk gel, the vapor, and the supported gel. As the  $F^-$  transport through the supported gel, it is also consumed during crystallization, leading to a lower concentration reaching the substrate surface than the original concentration of  $F^-$  in the bulk gel, which reduces the possibility of damaging the substrate. Also, unlike the traditional VPTM, the bulk gel is crystallized in the same reactor as the amorphous substrate; this allows the dry bulk gel to correctly mediate the amount of  $F^-$  that reaches the precursor film through the vapor phase. Using these protocols, well-adhered, continuous thin films of both the silicate, and the germanosilicate compositions of ITQ-29 (LTA) were prepared, on (100) Si, quartz, and glass substrates. These syntheses consistently (~ 95% of synthesis trials) yielded high-quality films with similar characteristics. Interestingly, these results suggest that the



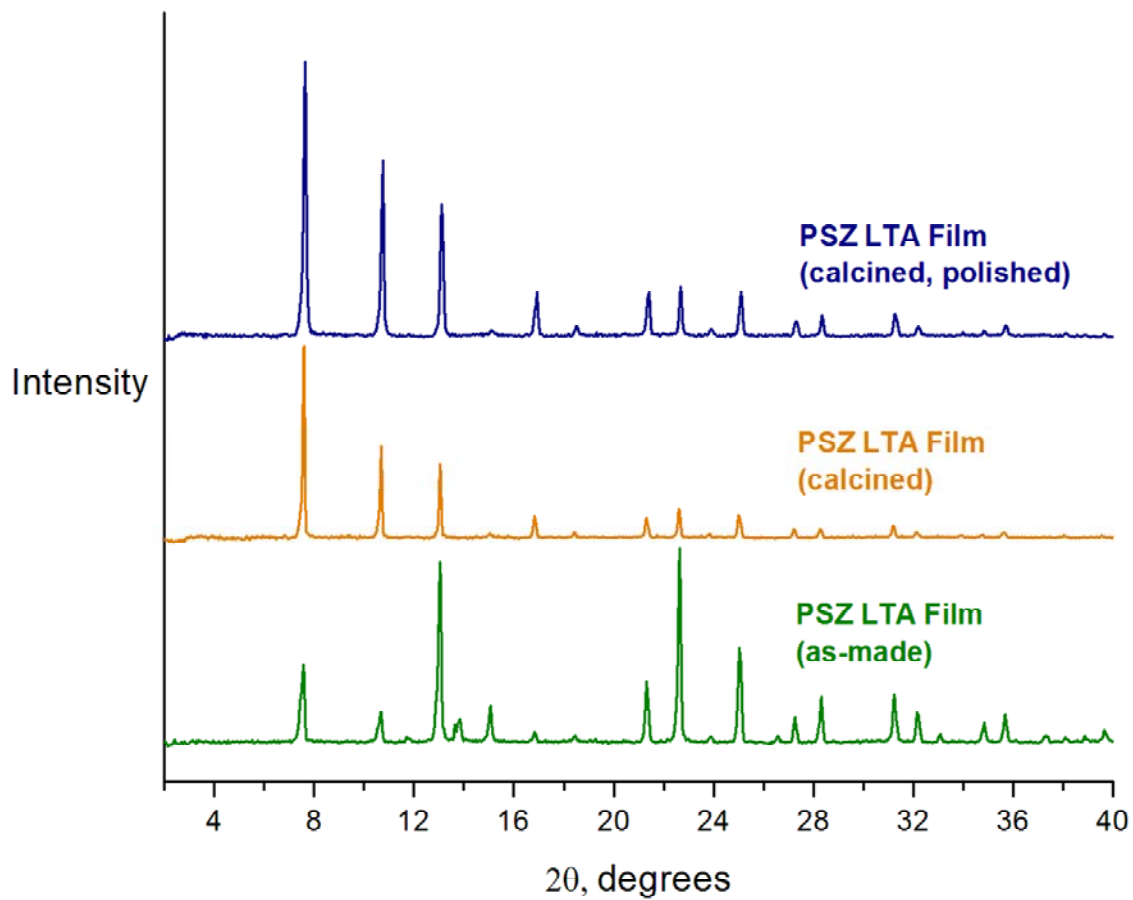
mechanism of film formation for this method is the crystallization of an amorphous gel coating on the surface of the support, as suggested by Myatt et al. and Kita et al.<sup>28,29</sup>

Post-synthesis, the ITQ-29 films were calcined and mechanically polished to create thin films in the range of 0.5 – 2  $\mu\text{m}$  thick for further characterization.

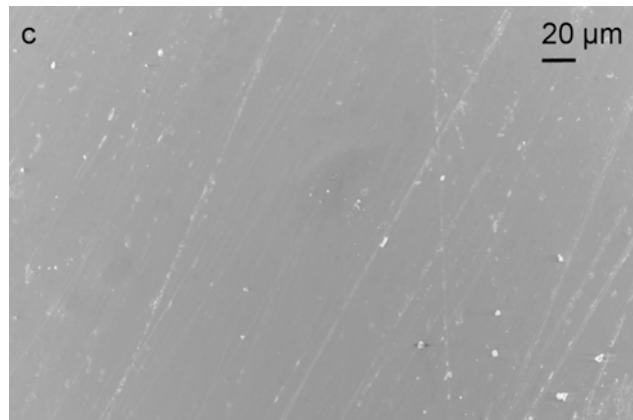
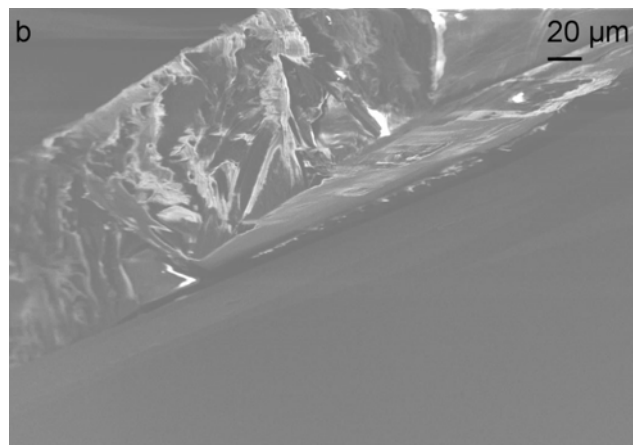
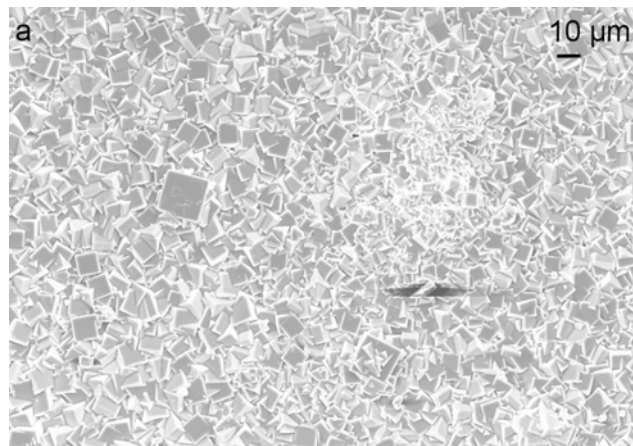
XRD patterns (Figure 3.6) show that the as-synthesized ITQ-29 films have pure LTA structure that is not affected by calcination and polishing. Micrographs, obtained via Field Emission Scanning Electron Microscopy (FE SEM), of a typical pure-silica ITQ-29 film show that the films are polycrystalline, intergrown, and continuous (Figure 3.7a), and are composed of cubic LTA crystals, (typical habit) ranging in size from less than 1  $\mu\text{m}$  to 20  $\mu\text{m}$ . Note that the films do not show evidence of cracking. Improper calcination (i.e., calcination at ramp rates faster than 1  $^{\circ}\text{C}$  / minute) result in cracked films due to the difference in thermal expansion of the substrate vs. the film itself. The ITQ-29 films on glass were calcined once to evaluate the effects of calcination.

Interestingly, the film did not crack, but rather bent as the substrate melted. Additionally, films that were not calcined for an appropriate length of time under air still exhibited the presence of the structure-directing agents in the pore system; for particularly thick films, this resulted in a grey coloration to the film. A thin section (Figure 3.7b) of the film indicates that the thickness can be increased up to  $\sim 115$   $\mu\text{m}$ , although thinner films are generally obtained by using fewer dip-coats during synthesis. A relatively smooth surface (Figure 3.7c) with an average thickness of 1.7  $\mu\text{m}$  (Fig. 3.7d) results from mechanically polishing the film. Interestingly, the LTA film syntheses tend to produce very regular crystals of its typical habit with the cubic face roughly normal to the substrate. This

suggests that zeolite crystal growth is more favorable in the direction that results in a high surface area contact with the substrate. Also interesting is that while the films could be produced with ease on quartz, glass, and (100) Si, we were unable to produce films on stainless steel or (111) Ge. The former was due to leaching of aluminum from the substrate during the film synthesis, which inhibits the growth of pure-silica zeolite LTA for the compositional regime discussed here, while the latter was due to a lattice mismatch between the substrate and the film, which prevented good adhesion to the substrate via typical bonding. The end results of this method are polycrystalline, intergrown, and continuous films on silicon-based substrates that can be polished to smooth surfaces.



**Figure 3.6** X-ray diffraction patterns of as-made, calcined and polished PSZ LTA film samples on OH-(100) Si demonstrates phase crystallization of the precursor film using the VPTM of fluoride



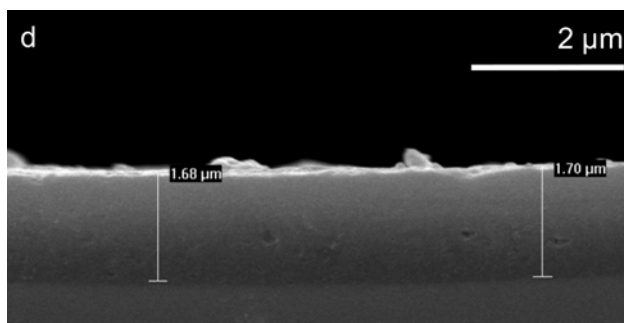


**Figure 3.7** FE SEM micrographs of (a) surface of calcined PSZ LTA film; (b) a thin section of calcined PSZ LTA film showing  $\sim 115 \mu\text{m}$  thick film; (c) surface of calcined PSZ LTA film after mechanical polishing; (d) a thin section of calcined PSZ LTA film after polishing showing  $\sim 1.7 \mu\text{m}$  thick film

Energy Dispersive X-ray Spectroscopy (EDS, Table 3.1) was used to show that the calcined, pure-silica LTA films are indeed pure-silica (66.65 atomic % O and 33.21 atomic % Si, with other elements (for example, carbon, tungsten, and vanadium, likely due to contaminants in the FE SEM) present in trace quantities), and that the SDA has been fully removed from the pores.

**Table 3.1** Energy dispersive spectrometry (EDS) data of the amorphous precursor film supported on OH-(100) Si demonstrates that the film is pure-silica, with the carbon content appearing due to the TMAOH and SDA in the precursor gel. EDS data for the calcined sample indicates that the carbon content has been completely removed.

	<b>Amorphous Precursor Film</b>			<b>Calcined Film</b>	
	<b>Si</b>	<b>O</b>	<b>C</b>	<b>Si</b>	<b>O</b>
<b>Weight %</b>	28.42	33.52	38.07	46.58	53.25
<b>Weight % <math>\sigma</math></b>	1.56	1.96	3.14	0.53	0.58
<b>Atomic %</b>	16.12	33.38	50.50	33.21	66.65

The average mechanical properties of the ITQ-29 films on low-resistivity (100) silicon wafers were evaluated (Figure 3.8). A mean elastic modulus of  $E = 49$  GPa ( $\sigma = 18$ ) was obtained for the samples via nanoindentation tests, which surpasses the minimum modulus ( $E > 6$  GPa) required for survival in the chemical and mechanical polishing process during integrated circuit fabrication. The reasons for the wide range in the modulus obtained from these nanoindentation measurements are currently unknown, but it is likely due to a combination of factors, including (1) the polycrystallinity of the film, whose grain boundaries may affect the compression tests, (2) the varying orientation of the crystals, since the mechanical properties of the crystals may be different for different orientations, and (3) the presence of some small crystals remaining on the surface after polishing, which will behave differently than a crystal fully imbedded in the film.

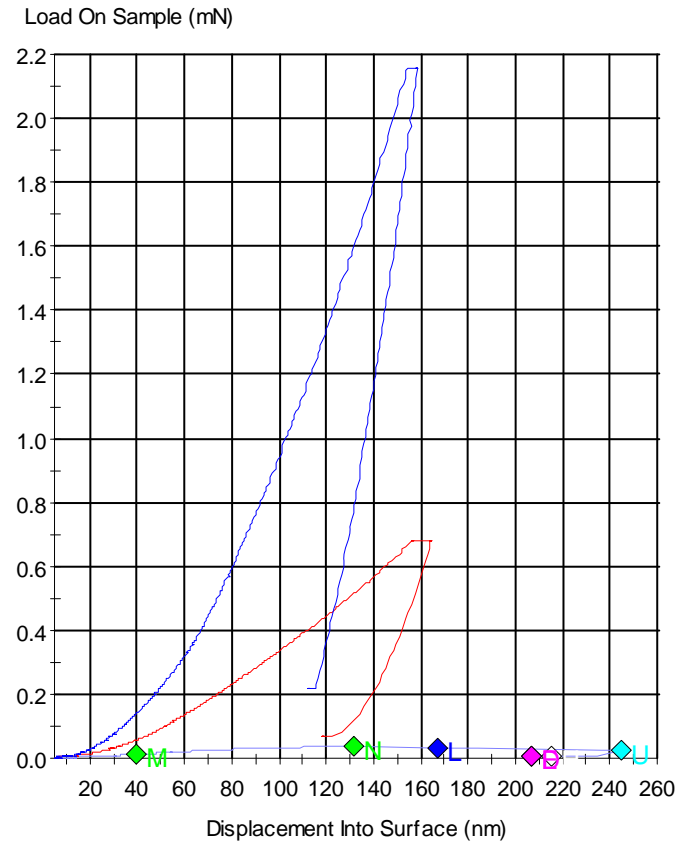


**Figure 3.8** Load / displacement curves for the PSZ ITQ-29 films on (100) Si wafers indicate that different elastic moduli are obtained at different indentation sites

### 3. Conclusions

We have examined two significant modifications to standard in situ film crystallization techniques: a seeding / diluting modification, and a vapor phase transport of the fluoride ion modification on the film synthesis of the ITQ-29 (LTA) zeolite. While the seeding / diluting modification did not yield ITQ-29 films, it did show that the acceptable composition range for producing ITQ-29 could be increased by the presence of pre-formed ITQ-29 seeds. This modification was particularly stymied by the degradation of the substrate due to direct contact with hydrofluoric acid in the synthesis. The second modification, which used the vapor phase transport method, eliminated the problems of contact with the hydrofluoric acid by transporting the fluoride via the vapor phase.

Therefore, we developed a new and general film deposition method that takes advantage of the vapor phase transport of the fluoride mineralizing agent. Specifically, we made a simple but significant modification of the Vapor Phase Transport Method (VPTM, for generating aluminosilicate membranes) by taking advantage of the volatility of the mineralizing agent and transporting it (not the solvent or SDA as in the traditional VPTM) via the vapor phase.<sup>30,31</sup> Using this method, we obtained well-adhered, continuous, and polycrystalline films of the pure-silica and germanosilica zeolites with LTA topology for the first time. This was a facile, reproducible, and general scheme for the production of fluoride-mediated, pure-silica zeolite films. The synthesis scheme may extend the current library of pure-silica zeolite films to include a wider range of topologies not obtainable via other synthetic methodologies. These materials could be beneficial to low-*k* dielectric applications, as well as catalytic and sensor applications.



Lastly, this method could result in other approaches to applications, such as ink-jet printing and patterning of films.

#### 4. Experimental

##### 4.1 Synthesis of Structure-Directing Agent (4-methyl-2,3,6,7-tetrahydro-1H,5H-pyrido [3.2.1-ij] quinolinium hydroxide)

10 g of julolidine (97%, Aldrich) was dissolved in 100 mL of  $\text{CHCl}_3$  (EMD). 24.5 g of  $\text{CH}_3\text{I}$  (99%, Aldrich) was then added and the resulting mixture was stirred at room temperature under Ar for three days. The addition of  $\text{CH}_3\text{I}$ , followed by stirring for three days, was repeated twice more. The solution was then quenched with 50 mL of double de-ionized (DDI)  $\text{H}_2\text{O}$ , and stirred for 30 min. The solvent was removed using a rotovap and the solids obtained were washed with ether and dried again using a rotovap. The crude product was recrystallized from 100 mL dichloromethane (EMD) at its boiling point and 50 mL of cold hexane (EMD). Pale yellow crystals of 4-methyl-2,3,6,7-tetrahydro-1H,5H-pyrido [3.2.1-ij] quinolinium iodide were obtained after vacuum drying the resulting solid;  $^{13}\text{C}$ -NMR of the product (300MHz,  $\text{D}_2\text{O}$ ,  $\delta$ ): 18.2, 25.8, 53.5, 65.9, 131.2, 132.0, 132.5, 141.0. The product (5.54 g, 17.6 mmol) was ion-exchanged from its iodide form to its hydroxide form by dissolution in 150 mL of DDI  $\text{H}_2\text{O}$  and stirring with 25.1 g of Bio-Rad AG1-X8 anion exchange resin for 24 h. The solution was then filtered and concentrated to 0.1 - 0.3 M concentration of the hydroxide form using a rotovap. The conversion from iodide to hydroxide was 95.2% based on titration of the resultant solution.

## 4.2 Synthesis of ITQ-29 (LTA) Films and Powder Via Seeding / Diluting

ITQ-29 (LTA) can be made with a germanosilicate, as well as a purely siliceous, composition. We attempted to synthesize films of each composition on a variety of substrates (low-resistivity (0.008 – 0.02  $\Omega$  cm), (100) silicon wafers (University Wafers), quartz wafers (University Wafers), glass microslides (Corning), sapphire wafers (University Wafers), and stainless steel. The pure-silica or germanosilicate precursor gel was prepared in a Teflon® jar by hydrolyzing tetraethylorthosilicate (TEOS, 98%, Aldrich) in an aqueous solution of SDA A and either tetramethylammonium hydroxide (TMAOH, 25%, Aldrich) for the pure-silica form or germanium (IV) oxide (GeO<sub>2</sub>, Alfa Aesar) for the germanosilicate form. The precursor gel of molar composition 1.0 TEOS / 0.13 TMAOH / 0.38 SDA / 50 H<sub>2</sub>O / 0 – 5 wt % seeds (pure-silica gel) or 0.67 TEOS / 0.247 GeO<sub>2</sub> / 0.6 SDA / 50 H<sub>2</sub>O / 0-5 wt % seeds (germanosilicate gel), on a 1.000 g TEOS basis, was stirred for 26 h at room temperature to ensure complete hydrolysis of TEOS. A Teflon® cap with two small holes drilled in it was screwed onto the jar containing the bulk precursor gel. The enclosed bulk precursor gel was placed inside a vacuum desiccator, and the ethanol and excess H<sub>2</sub>O present in the bulk precursor gel and precursor film were evaporated. Evacuation for 48 h at room temperature yielded a solid (dry) bulk gel of molar composition 1.0 SiO<sub>2</sub> / 0.13 TMAOH / 0.38 SDA / 2.0 H<sub>2</sub>O / 0 – 5 wt % seeds (for the pure-silica form) or .67 TEOS / 0.247 GeO<sub>2</sub> / 0.6 SDA / 7.0 H<sub>2</sub>O / 0 - 5 wt % seeds (for the germanosilicate form). The gel was then diluted to the final water concentration, an aqueous solution of hydrofluoric acid (48%, Mallinckrodt) was added to the jar in molar ratio 0.50 HF / 1.0 SiO<sub>2</sub> (pure-silica form) or 0.60 HF / 0.67 SiO<sub>2</sub> (germanosilicate form), and the sample was stirred with a Teflon® spatula. The dry bulk

gel, followed by a 4 cm x 2 cm substrate cleaned of organics via an HF etch, was introduced into a Teflon®-lined Parr Autoclave. The crystallization was carried out at 135 °C (pure-silica form) or at 150 °C (germanosilicate form) for 7 – 20 days. The reactor was removed from the oven and cooled. The bulk solids and the substrate were washed with 100 mL each of acetone (EMD) and DDI H<sub>2</sub>O. The crystalline material was placed in an evaporating dish and dried for 24 h in a 100 °C oven. The organic SDA was removed from the powder samples by calcination in air at 700 °C for 5 h using a ramp rate of 2 °C / min, with pauses at 350 °C and 580 °C for 3 h each.

#### 4.3 Synthesis of ITQ-29 (LTA) Films and Powder Via Vapor Phase Transport of Fluoride

ITQ-29 (LTA) can be made with a germanosilicate, as well as a purely siliceous, composition. We synthesized films of each composition on a variety of substrates (low-resistivity (0.008 – 0.02 Ω cm), (100) silicon wafers (University Wafers), quartz wafers (University Wafers), and glass microslides (Corning). These substrates were modified to present Si-OH terminal groups on their surface by soaking in a piranha-type etch solution, i.e., 10 mL H<sub>2</sub>SO<sub>4</sub> (97%, J.T. Baker) : 40 mL H<sub>2</sub>O<sub>2</sub> (30%, EMD) : 2 drops of HF (48%, Mallinckrodt), for 2 min, followed by 15 min in DDI H<sub>2</sub>O [29]. The pure-silica or germanosilicate precursor gel was prepared in a Teflon® jar by hydrolyzing tetraethylorthosilicate (TEOS, 98%, Aldrich) in an aqueous solution of SDA A and either tetramethylammonium hydroxide (TMAOH, 25%, Aldrich) for the pure-silica form or germanium (IV) oxide (GeO<sub>2</sub>, Alfa Aesar) for the germanosilicate form. A 4 cm x 2 cm, previously modified substrate was then submerged in the gel. The precursor gel of molar

composition 1.0 TEOS / 0.13 TMAOH / 0.38 SDA / 50 H<sub>2</sub>O (pure-silica gel) or 0.67 TEOS / 0.247 GeO<sub>2</sub> / 0.6 SDA / 50 H<sub>2</sub>O (germanosilicate gel), on a 1.000 g TEOS basis, was stirred for 26 h at room temperature to ensure complete hydrolysis of TEOS. The submerged substrate was thereafter removed from the gel, and subjected to dip-coating up to five times in the hydrolyzed gel, with 30 min of drying on a Teflon® substrate holder at room temperature between coats. This created an amorphous precursor film on the substrate. A Teflon® cap with two small holes drilled in it was screwed onto the jar containing the bulk precursor gel. The coated substrate, in its holder, and the enclosed bulk precursor gel were each placed inside a vacuum desiccator, and the ethanol and excess H<sub>2</sub>O present in the bulk precursor gel and precursor film were evaporated. Evacuation for 48 h at room temperature yielded an amorphous precursor film and a solid (dry) bulk gel of molar composition 1.0 SiO<sub>2</sub> / 0.13 TMAOH / 0.38 SDA / 2.0 H<sub>2</sub>O (for the pure-silica form) or .67 TEOS / 0.247 GeO<sub>2</sub> / 0.6 SDA / 7.0 H<sub>2</sub>O (for the germanosilicate form). If, after drying, too much H<sub>2</sub>O had been removed, DDI H<sub>2</sub>O was added to the jar to obtain the correct total gel mass. An aqueous solution of hydrofluoric acid (48%, Mallinckrodt) was added to the jar in molar ratio 0.50 HF / 1.0 SiO<sub>2</sub> (pure-silica form) or 0.60 HF / 0.67 SiO<sub>2</sub> (germanosilicate form) and the sample was stirred with a Teflon® spatula. The dry bulk gel, followed by the coated substrate on an elevated Teflon® platform, was introduced into a Teflon®-lined Parr Autoclave. The crystallization of the bulk gel and the precursor films for 20 days was carried out at 135 °C (pure-silica form) or at 150 °C (germanosilicate form). The reactor was removed from the oven and cooled. The bulk solids and the film were washed with 100 mL each of acetone (EMD) and DDI H<sub>2</sub>O. The crystalline material was placed in an evaporating

dish and dried for 24 h in a 100 °C oven. The organic SDA was removed from the powder and film samples by calcination in air at 700 °C for 5 h using a ramp rate of 1 °C / min, with pauses at 350 °C and 580 °C for 3 h each.<sup>17</sup>

#### 4.4 Characterization

The chemicals synthesized to produce the zeolite precursor gels were characterized using a combination of liquid-state <sup>1</sup>H and <sup>13</sup>C NMR with a Varian Mercury 300 MHz spectrometer. The as-made and calcined zeolite samples were evaluated using powder X-ray diffraction (XRD) on a Scintag XDS 2000 diffractometer operated at -40 kV and 40 mA using Cu K<sub>α</sub> radiation ( $\lambda = 1.54056 \text{ \AA}$ ) and a solid-state Ge detector in the 2 $\theta$  range of 2-40 at a step size of 0.5 ° / min. TGA was performed on a NETZSH STA 449C analyzer in air using an aluminum sample pan at a rate of 5 °C / min. All FE SEM was done on a LEO 1550 VP FE SEM at an electron high tension (EHT) of 10 kV using samples that were coated, using a metal sputtering coater, with 5 nm of Pt to minimize the effects of charging. EDS measurements were carried out using an Oxford INCA Energy 300 EDS system. Elastic modulus and hardness measurements for the pure-silica zeolite LTA films on (100) Si were obtained via nanoindentation with an Agilent Corp. Nanoindenter G200 using a Berkovich diamond punch, a strain rate of 0.050, an indentation depth of 150 nm, and a Poisson ratio of 0.329, obtained via averaging data from Hazen et al. on the compressibility of zeolite LTA.<sup>12,32,33,34,35</sup> The calcined films were mechanically polished using a Buehler EComet 3000 Polisher equipped with 0.05  $\mu\text{m}$  Al<sub>2</sub>O<sub>3</sub> polishing suspension and a 3  $\mu\text{m}$  abrasive lapping film.

## 5. References

- <sup>1</sup> Davis, M. E. Ordered porous materials for emerging applications. *Nature* **417**, 813-821 (2002).
- <sup>2</sup> Caro, J. & Noack, M. Zeolite membranes - Recent developments and progress. *Microporous Mesoporous Mat.* **115**, 215-233 (2008).
- <sup>3</sup> McLeary, E. E., Jansen, J. C. & Kapteijn, F. Zeolite based films, membranes and membrane reactors: Progress and prospects. *Microporous Mesoporous Mat.* **90**, 198 (2006).
- <sup>4</sup> Bein, T. Synthesis and applications of molecular sieve layers and membranes. *Chem. Mater.* **8**, 1636-1653 (1996).
- <sup>5</sup> Mintova, S. & Bein, T. Nanosized zeolite films for vapor-sensing applications. *Microporous Mesoporous Mat.* **50**, 159-166 (2001).
- <sup>6</sup> Yan, Y. G. & Bein, T. Molecular Recognition Through Intercalation Chemistry - Immobilization Of Organoclays On Piezoelectric Devices. *Chem. Mater.* **5**, 905-907 (1993).
- <sup>7</sup> Yan, Y. G. & Bein, T. Molecular Recognition On Acoustic-Wave Devices - Sorption In Chemically Anchored Zeolite Monolayers. *J. Phys. Chem.* **96**, 9387-9393 (1992).
- <sup>8</sup> Bein, T. *et al.* Microporous Assemblies For Chemical Recognition - Zeolite Layers And Sol-Gel-Derived Glass-Films On Sensors. *Abstr. Pap. Am. Chem. Soc.* **204**, 161-COLL (1992).
- <sup>9</sup> Salomon, M. A., Coronas, J., Menendez, M. & Santamaria, J. Synthesis of MTBE in zeolite membrane reactors. *Appl. Catal. A-Gen.* **200**, 201-210 (2000).

- <sup>10</sup> *International Technology Roadmap for Semiconductors* (2007).
- <sup>11</sup> Maex, K. *et al.* Low dielectric constant materials for microelectronics. *J. Appl. Phys.* **93**, 8793-8841 (2003).
- <sup>12</sup> Li, Z. J. *et al.* Mechanical and dielectric properties of pure-silica-zeolite low-k materials. *Angew. Chem.-Int. Edit.* **45**, 6329-6332 (2006).
- <sup>13</sup> Morgen, M. *et al.* Low dielectric constant materials for ULSI interconnects. *Annu. Rev. Mater. Sci.* **30**, 645-680 (2000).
- <sup>14</sup> Yan, Y., Wang, Z. & Wang, H. *Silica Zeolite Low-K Dielectric Thin Films*. U.S. Patent #6573131 (2003).
- <sup>15</sup> Wang, Z. B., Wang, H. T., Mitra, A., Huang, L. M. & Yan, Y. S. Pure-silica zeolite low-k dielectric thin films. *Adv. Mater.* **13**, 746-749 (2001).
- <sup>16</sup> Corma, A., Rey, F., Rius, J., Sabater, M. J. & Valencia, S. Supramolecular self-assembled molecules as organic directing agent for synthesis of zeolites. *Nature* **431**, 287-290 (2004).
- <sup>17</sup> Tiscornia, I. *et al.* Preparation of ITQ-29 (Al-free zeolite a) membranes. *Microporous Mesoporous Mat.* **110**, 303-309 (2008).
- <sup>18</sup> Liu, Y., Sun, M. W., Lew, C. M., Wang, J. L. & Yan, Y. S. MEL-type pure-silica zeolite nanocrystals prepared by an evaporation-assisted two-stage synthesis method as ultra-low-k materials. *Adv. Funct. Mater.* **18**, 1732-1738 (2008).
- <sup>19</sup> Mitra, A. *et al.* Synthesis and evaluation of pure-silica-zeolite BEA as low dielectric constant material for microprocessors. *Ind. Eng. Chem. Res.* **43**, 2946-2949 (2004).

- 20 Hu, L. L., Wang, J. L., Li, Z. J., Li, S. & Yan, Y. S. Interfacial adhesion of  
nanoporous zeolite thin films. *J. Mater. Res.* **21**, 505-511 (2006).
- 21 Cho, Y. Pure Silica Zeolite Films Prepared by a Vapor Phase Transport Method.  
*Japanese Journal of Applied Physics, Parts 1 & 2* **47**, 8360-8363 (2008).
- 22 Chen, Y. L. *et al.* Synthesis and characterization of pure-silica-zeolite Beta low-k  
thin films. *Microporous Mesoporous Mat.* **123**, 45-49,  
doi:10.1016/j.micromeso.2009.03.022 (2009).
- 23 Zones, S. I. *et al.* The fluoride-based route to all-silica molecular sieves; a  
strategy for synthesis of new materials based upon close-packing of guest-host  
products. *Comptes Rendus Chimie* **8**, 267-282 (2005).
- 24 Corma, A. & Davis, M. E. Issues in the synthesis of crystalline molecular sieves:  
Towards the crystallization of low framework-density structures. *ChemPhysChem*  
**5**, 304-313 (2004).
- 25 Bouizi, Y., Paillaud, J. L., Simon, L. & Valtchev, V. Seeded synthesis of very  
high silica zeolite A. *Chem. Mater.* **19**, 652-654 (2007).
- 26 Matsukata, M. & Kikuchi, E. Zeolitic membranes: Synthesis, properties, and  
prospects. *Bull. Chem. Soc. Jpn.* **70**, 2341-2356 (1997).
- 27 Mitra, A., Ichikawa, S., Kikuchi, E. & Matsukata, M. Hydrovapo-thermal  
conversion of tetraethoxysilane vapor to polycrystalline zeolite layer by in situ  
gelation. *Chem. Commun.*, 900-901 (2004).
- 28 Myatt, G. J., Budd, P. M., Price, C. & Carr, S. W. Synthesis of a Zeolite NaA  
Membrane. *J. Mater. Chem.* **2**, 1103-1104 (1992).



- <sup>29</sup> Kita, H., Horii, K., Ohtoshi, Y., Tanaka, K. & Okamoto, K. I. Synthesis of a Zeolite NaA Membrane for Pervaporation of Water-Organic Liquid-Mixtures. *J. Mater. Sci. Lett.* **14**, 206-208 (1995).
- <sup>30</sup> Kim, M. H., Li, H. X. & Davis, M. E. Synthesis of zeolites by water-organic vapor-phase transport. *Microporous Mater.* **1**, 191-200 (1993).
- <sup>31</sup> Brinker, C. J. Evaporation-induced self-assembly: Functional nanostructures made easy. *MRS Bull.* **29**, 631-640 (2004).
- <sup>32</sup> Johnson, M., Li, Z. J., Wang, J. L. & Yan, Y. S. Mechanical characterization of zeolite low dielectric constant thin films by nanoindentation. *Thin Solid Films* **515**, 3164-3170 (2007).
- <sup>33</sup> Xiang, Y., Chen, X., Tsui, T. Y., Jang, J. I. & Vlassak, J. J. Mechanical properties of porous and fully dense low-kappa dielectric thin films measured by means of nanoindentation and the plane-strain bulge test technique. *J. Mater. Res.* **21**, 386-395 (2006).
- <sup>34</sup> Hazen, R. M. Zeolite Molecular-Sieve 4a - Anomalous Compressibility And Volume Discontinuities At High-Pressure. *Science* **219**, 1065-1067 (1983).
- <sup>35</sup> Hazen, R. M. & Finger, L. W. Compressibility Of Zeolite-4a Is Dependent On The Molecular-Size Of The Hydrostatic-Pressure Medium. *J. Appl. Phys.* **56**, 1838-1840 (1984).